Journal of Molecular Structure, 74 (1981) 233—253
Elsevier Scientific Publishing Company, Amsterdam — Printed in The Netherlands

CONFORMATION AND VIBRATIONAL SPECTRA OF 1,5-HEXADIYNE (BIPROPARGYL) AND 1,5-HEXADIYNE-1,6-d_2

G. O. BRAATHEN, C. J. NIELSEN and P. KLAEBOE

Department of Chemistry, University of Oslo, Oslo 3 (Norway)

H. HOPF

Institute of Organic Chemistry, The Technical University of Braunschweig, D-3300, Braunschweig (W. Germany)

(Received 30 January 1981)

ABSTRACT

The infrared spectra of 1,5-hexadiyne (bipropargyl) and 1,5-hexadiyne-1,6-d_2 as vapours, liquids, as solutes in various solvents and as crystalline solids at low temperatures and at high pressures have been recorded. Raman spectra were obtained for the liquids, including semiquantitative polarization measurements, and for the low temperature crystals.

The data were interpreted in terms of two conformers, *anti* and *gauche*, in the vapour and liquid state and one, the *anti*, in the crystalline forms. A phase transition for 1,5-hexadiyne was observed at ca. 240 K. Both the high and low temperature crystals had molecules in the *anti* conformer.

Interpretation of the spectra in terms of conformational equilibria was facilitated by a thorough vapour phase band contour analysis. With a few exceptions, all the vibrational fundamentals for both conformers were assigned and found to be in good agreement with results from normal coordinate calculations.

INTRODUCTION

The infrared and Raman spectra of 1,5-hexadiyne (bipropargyl, abbreviated to BP in this paper) were studied in our laboratories a few years ago [1], while the C—H stretching region was independently investigated [2] to evaluate the hydrogen bonding in the liquid state and in solution. Our results revealed that BP exists as an equilibrium of two conformers in the vapour phase, in the liquid and in solution. The more abundant conformer in these phases was present alone in the crystalline solid at 90 K [1].

With some doubt we concluded from the spectra that the more stable conformer was *anti*, later verified by the results from gaseous electron diffraction [3]. However, the spectra of BP were difficult to interpret, since a number of accidental degeneracies and fundamentals coinciding with combination modes of the opposite conformer, among others, occurred. The *gauche* spectrum was particularly difficult to analyze since the bands were often weak and superposed on the frequently more intense *anti* bands.

Thus, we decided to repeat the spectral work on BP, and a deuterated compound i.e. 1,5-hexadiyne-1,6-d_2 (hereinafter called BP-d_2) was also synthesized and studied. In addition, various other spectral features are emphasized in the present study: (1) an improved band contour analysis of *anti* and *gauche* bands was carried out, (2) the CH_2 stretching band intensities were estimated, (3) improved far IR spectra were obtained including spectra of the low temperature crystals below 200 cm^{-1}, (4) a more extensive force field was derived for BP and BP-d_2, (5) the solid state spectra were carefully studied in the temperature range 200—270 K and (6) infrared high pressure spectra were recorded at ambient temperature.

Further information for the spectral interpretations was provided by the recent results for related compounds such as hexa-1,2-diene-5-yne [4], 1,6-dibromo-1,5-hexadiyne [5], 1-bromo-1,5-hexadiyne [6] and 1-cyano-3-butyne [7].

EXPERIMENTAL

The sample of BP used in the present study was partly leftover from the earlier study [1] and partly a commercial sample from K & K. Both samples were dried with molecular sieves and subsequently distilled, and gas chromatographic analyses revealed high purities. In a 1 m gas cell, however, some very small discrepancies between their IR spectra were detected by expanding the ordinate scale (using the FT-IR spectrometer) and these peaks were ascribed to impurities.

For the preparation of 1,6-dideuterio-1,5-hexadiyne, 7.8 g (0.1 mol) BP in 50 ml of dry tetrahydrofuran was added under nitrogen to 200 ml of a well-stirred 0.3 m solution of ethylmagnesium bromide in tetrahydrofuran (prepared from 7.3 g (0.3 mol) magnesium turnings and 34.9 g (0.32 mol) of freshly distilled ethyl bromide), and the mixture stirred overnight. To complete the exchange, the solution was subsequently refluxed for 2 h and then decomposed with an excess of D_2O. Extraction with ether provided the BP-d_2 which was purified by preparative gas chromatography (6m-Carbowax, 65 C). The NMR and IR spectra of the sample showed it to be essentially free of acetylenic hydrogen.

Infrared spectra were recorded on a Perkin-Elmer model 225 spectrometer (5000—200 cm^{-1}) and on a Bruker IFS-114C Fourier transform spectrometer (4000—20 cm^{-1}). Spectra were recorded of the neat liquid, of C_6H_6 solutions and of the solid at ca. 90 K before and after annealing. Further spectra of the solid were recorded in the temperature region 200—270 K. Vapour spectra at various pressures were recorded at ambient temperature in 10 cm, 20 cm and 1 m cells equipped with windows of CsI, polyethylene and KRS 5, respectively. For the high pressure experiments a cell with type II diamonds was used with a 4X beam condenser and the spectra recorded on the interferometer [8].

Raman spectra were recorded with a modified [9] Cary 81 spectrometer

excited by a CRL model 52G argon ion laser. Spectra of the liquid, including semiquantitative polarization measurements, were obtained from ampoules sealed under vacuum; spectra of the crystalline solid at ca. 90 K were obtained from samples deposited on a copper block at 80 K and annealed to ca. 210 K.

RESULTS

Various IR and Raman spectra of BP in different phases have been reported [1] and the spectra are not repeated here. Corresponding spectra for BP-d_2 are given, showing the IR vapour (Fig. 1), liquid (Fig. 2) and crystalline solid (Fig. 3) spectra. Raman spectra of BP-d_2 as a liquid and as a crystalline solid are shown in Figs. 4 and 5, respectively. Additional far IR curves of the

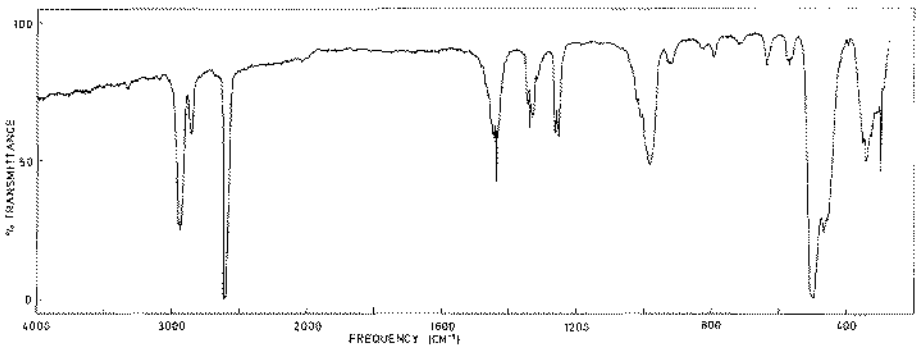

Fig. 1. The infrared spectrum of 1,5-hexadiyne-1,6-d_2 (BP-d_2) in the vapour phase, 10 cm cell, 45 torr pressure.

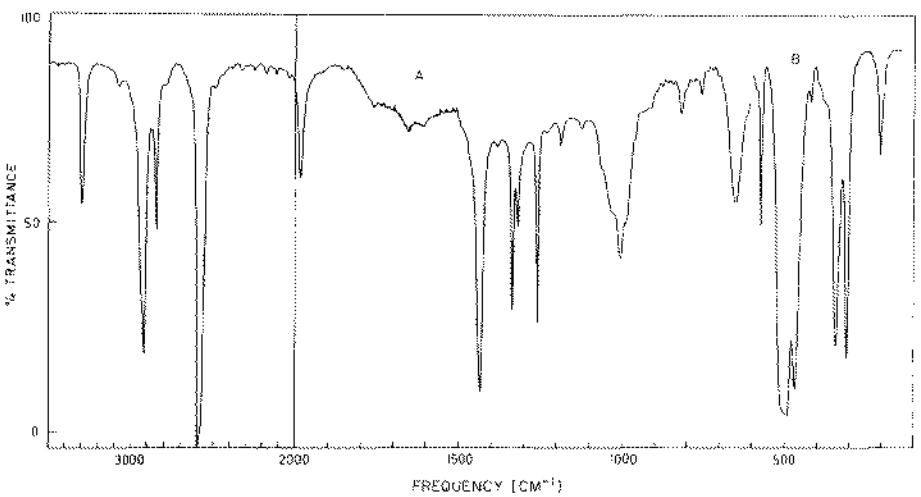

Fig. 2. The infrared spectrum of BP-d_2; A, neat liquid in 0.025 mm cell; B, 0.7% solution in benzene, 1 mm cell.

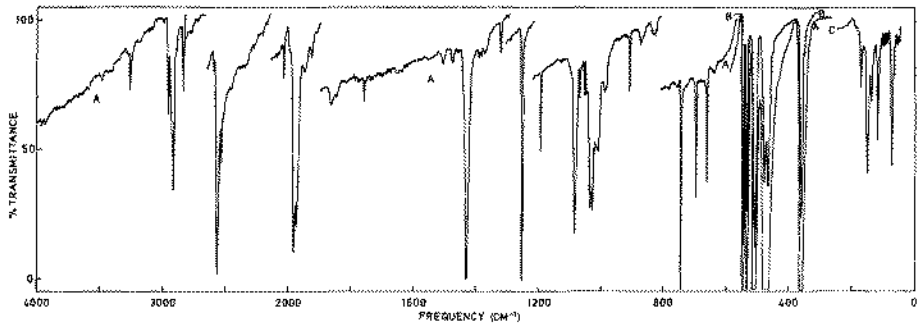

Fig. 3. The infrared spectrum of BP-d_2 at 90 K after annealing to ca. 190 K.

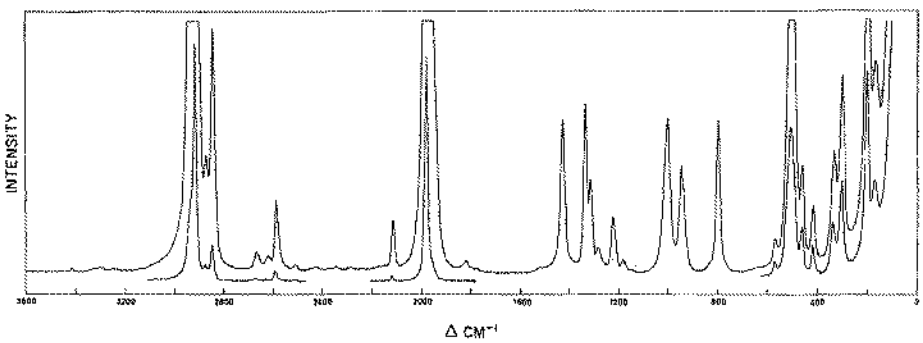

Fig. 4. The Raman spectrum of BP-d_2 in the liquid phase.

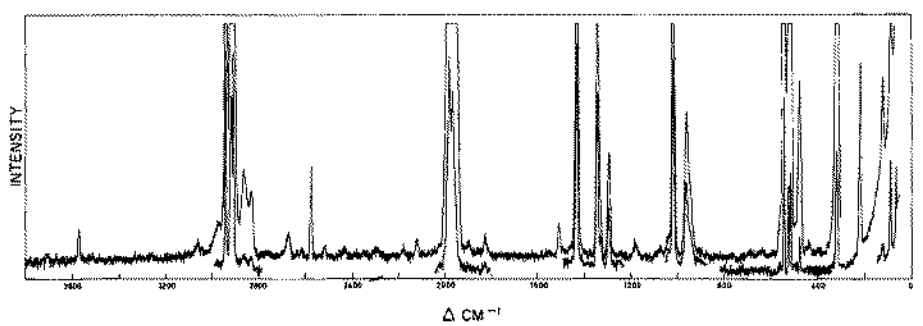

Fig. 5. The Raman spectrum of BP-d_2 at 90 K after annealing to ca. 190 K.

unannealed and the annealed crystalline solids at 90 K deposited on the window of silicon are shown in Figs. 6 (BP) and 7 (BP-d_2).

The wave numbers of the observed IR and Raman bands are listed in Tables 1 (BP) and 2 (BP-d_2) whereas the assigned fundamentals are listed in Tables 3 (BP) and 4 (BP-d_2).

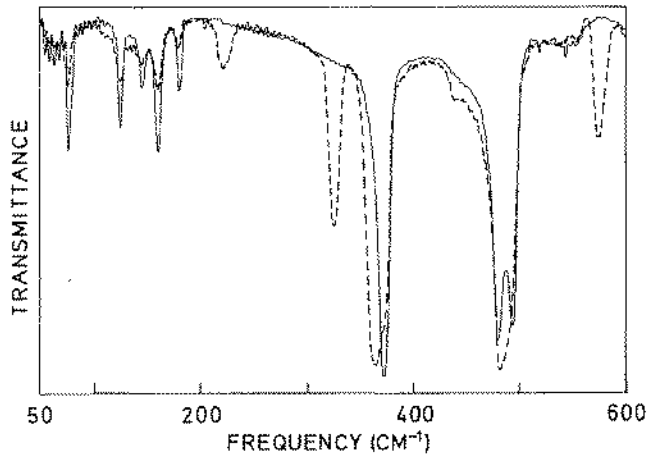

Fig. 6. The far infrared spectrum of 1,5-hexadiyne (BP) at 190 K; dotted line, amorphous solid; solid line, annealed crystalline phase.

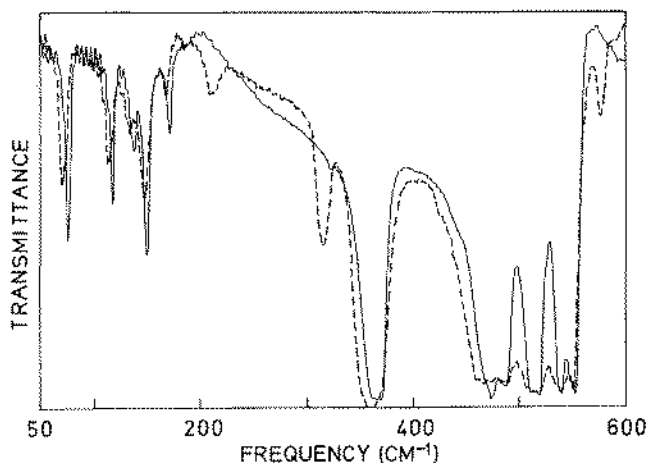

Fig. 7. The far infrared spectrum of BP-d_2 at 90 K; dotted line, amorphous solid; solid line, annealed crystalline solid.

Infrared vapour band contours

The structures of the *anti* and *gauche* conformers of BP have been determined by electron diffraction [3]. From the method outlined by Ueda and Shimanouchi [10] the band contours were calculated. The three theoretical vapour curves (*A*, *B* and *C* type contours) of the *anti* and *gauche* conformers, both being asymmetric tops are given in Figs. 8 and 9, respectively. As is apparent from Fig. 8, the *A*-type bands of the *anti* conformer have a *PR* separation of ca. 9 cm^{-1} and a weak central *Q*-branch. The *B*-type bands have two intense *Q*-branches separated by ca. 10 cm^{-1} with the *P* and *R* branches

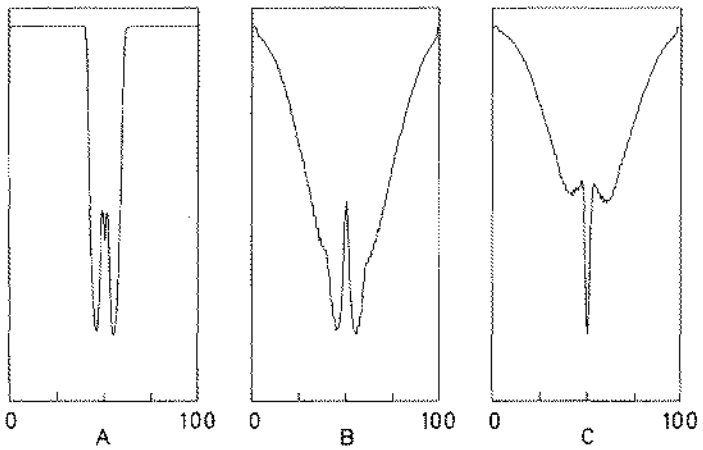

Fig. 8. Predicted vapour contours for *A*, *B* and *C* type bands of the *anti* conformer of BP.

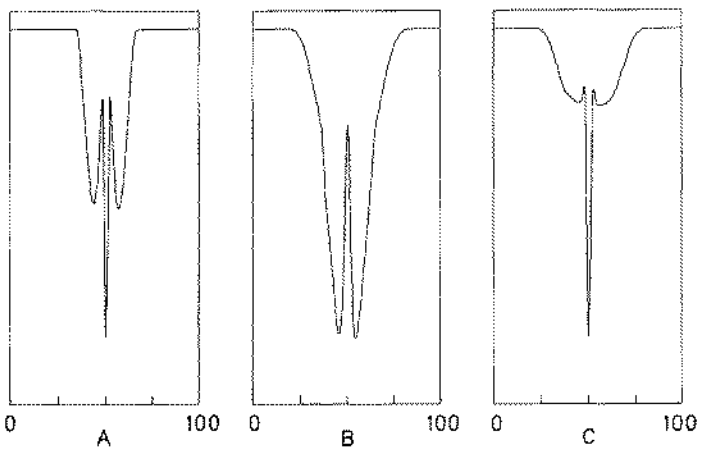

Fig. 9. Predicted vapour contours for the *A*, *B* and *C* type bands of the *gauche* conformer of BP.

appearing as medium intense shoulders. For the *C*-type bands a strong central *Q*-branch and medium intense *P* and *R* branches separated by ca. 23 cm^{-1} are expected.

For the *gauche* conformer (Fig. 9) we expect "normal" *A*-type bands with *PR* separations of ca. 14 cm^{-1}; the *B*-type bands consist of two intense *Q*-branches separated by ca. 9 cm^{-1} with very weak *P* and *R* shoulders, the *C*-type bands appear with a very intense central *Q*-branch and weak *P* and *R* branches separated by ca. 17 cm^{-1}. These accurately determined vapour contours deviate considerably from those predicted previously for BP [1] based upon standard procedures [11].

The a_u modes of the *anti* conformer will have *C*-type contours and the b_u modes *A/B* hybrid contours. For the *gauche* conformer the *a* modes should have *B*-type contours and the *b* modes *A/C* hybrid contours.

In conclusion it can be predicted that: (1) IR vapour bands with a central *Q*-branch and a *PR* separation of 23 cm^{-1} should belong to the a_u species (*anti*), whereas (2) a sharp central *Q*-branch and *PR* separation of 14 cm^{-1} indicate species *b* (*gauche*). (3) Bands with two branches separated by approximately 10 cm^{-1} can be either b_u (*anti*) or *a* (*gauche*). However, these bands may be identified by the Raman polarization measurements. The present results are in excellent agreement with our experimental IR vapour curves and were of great help in the assignments.

Infrared CH_2 stretching band intensities

With two methylene groups in the molecule, BP (and BP-d_2) should have two IR active stretching modes ν_{11} (a_u) and ν_{22} (b_u) of *anti* and four of the *gauche* conformer (ν_1, ν_2 of species *a* and ν_{17}, ν_{18} of species *b*) (numbered for BP-d_2). The spectra reveal that these bands overlap considerably in the region 3000—2900 cm^{-1}.

We expect three *Q*-branches, ν_{11} *anti* (*C*-type) and ν_{17} and ν_{18}, *gauche* (*A/C* hybrid). Three *Q*-branches were observed at 2932, 2956 and 2964 cm^{-1}; the 2956 cm^{-1} band is the most intense and was assigned as ν_{11}, *anti*, and the other two as ν_{17} and ν_{18} (*gauche*). Figure 10 (showing the methylene stretching region of BP-d_2) shows at least one additional band, apparently of *B*-type, between 2932 and 2956 cm^{-1}.

To facilitate the spectral interpretation the relative band intensities were estimated. For localized normal vibrations such as CH_2 stretch, the relative band intensities can be predicted from the *L*-matrix if the bond moment $(\partial\mu/\partial r)$ is constant [12]. The calculated relative intensities of the six IR active CH_2 stretching bands are listed in Table 5. Three bands without sharp *Q*-branches ν_{22} (b_u), ν_1 (*a*) and ν_2 (*a*) were assumed to be situated at 2943, 2969 and 2934 cm^{-1}, respectively, to make the best fit in the band contour analysis. The band intensities were added and the *anti/gauche* concentration ratio in the vapour phase estimated to be 5:1 (within the limits determined [3]). The constructed IR intensity curve is shown in Fig. 11 and gives fair agreement with the experimental curve (Fig. 10). Additional weak components of combination bands may contribute to the latter curve.

Spectral assignments in BP

We were previously [1] reluctant to make a very firm conclusion regarding which conformer was present in the crystalline phase, although it was assumed to be *anti*. The four relatively weak IR bands in BP at 1340, 571, 312 and 204 cm^{-1} present in the amporphous spectrum at 90 K disappeared after annealing (Fig. 6). In the vapour phase these bands all had *A/C* hybrid contours with a *PR* separation of 14 cm^{-1}. Therefore, they were *gauche* bands of species *b* and assigned as ν_{22}, ν_{28}, ν_{29} and ν_{30}. The latter two modes

TABLE 1

IR and Raman spectral data[a] for 1,5-hexadiyne (bipropargyl)

IR				Raman		Interpretation	
Vapour	Liquid	Amorphous[b] 90 K	Crystalline[c] 90 K	Liquid	Crystalline[c] 90 K	*Anti*	*Gauche*
3374m,sh[d]						$\nu_9 + \nu_{23}$	
3337vs			3264vs		3270s		
3332vs *A/B*	3301vs	3262vs		3299m,P		ν_{22}, ν_1	ν_1, ν_{17}
3326vs			3248m		3258s		
3314ms							
B						$\nu_3 + \nu_{26}$	
3306ms							
					3050w	$\nu_3 + \nu_7$	
2971m,sh							
2964s,Q *A/C*	2946m,sh						ν_{16}
2959s							
			2955s				
2956s,Q *C*	2935m,sh	2935m,sh		2938s,sh,D	2942vs	ν_{11}, ν_{17}	
			2933ms				
2945s							
2951s					2922s		
B	2921s	2918s	2917s	2921vs,P		ν_{23}, ν_2	
2939s					2912vs		
2932s,Q *A/C*							ν_{19}
2926m,sh							
2872m							
2866m *B*				2875w,P	2864m	$\nu_{13} + \nu_{24}$	
	2849m	2843m	2837m			$\nu_4 + \nu_{25}$	
2863m *A/C*				2849m,P	2832m	$2\nu_4, 2\nu_{25}$	
2861m							
	2150w,sh						$\nu_{22} + \nu_{25}$
2140m				2134w,sh			
					2119vs		
2138m *A/B*	2121m	2118m	2116mw	2118vs,P		ν_{24}, ν_3	ν_4, ν_{20}
2130m					2115vs		
	1473m,sh					$\nu_{10} + \nu_{26}$	
1447m	1441s,sh		1431s	1436m,P	1431s	ν_{25}, ν_4	
1441s,Q *A/C*	1435s	1439s					ν_5, ν_{21}
1435m							
			1412m			Comb. of	
			1392m			crystal	
			1383m			inter-	
			1344m			actions	
			1315m		1345s		
				1346m,P		ν_5	
					1334s		
1348m						$\nu_{15} + \nu_{19}$	
1343m							ν_{22}
1340m *A/C*	1338ms	1345m					
1334m							
B	1321ms	1317m		1322wm,P	*[e]		ν_6
1322wm							
1317w							
1273s,sh							
	1290ms,br	1297ms,sh	1295m	1286w,D	1293ms	comb., ν_{18}	
1267s,Q							
1263s			1256s				
B	1260s	1259s				ν_{26}	
1255s			1252m				
	1228m,sh		*	1225mw,P	*		ν_7

TABLE 1 (continued)

IR				Raman		Interpretation	
Vapour	Liquid	Amorphous[b] 90 K	Crystalline[c] 90 K	Liquid	Crystalline[c] 90 K	*Anti*	*Gauche*
1191 vw,Q *C*	1189 wm	1188 m	1196 m			ν_{12}	
1187 vw							
1184 vw							
1181 vw,Q *A/C*				1187 vw,D			ν_{23}
1071 vw	1079 w	1075 w	1072 w			$\nu_{13} + \nu_{21}$	
				1030 s,sh,D			ν_8 ?
	1024 vw	1022 vw		1022 s,P	1022 s	ν_6	
1010 vw }							
B	1002 wm	1002 w	*	1003 m,P	1007 w	ν_{19}	ν_9
1000 vw }							
974 vw,Q	970 w	975 w	976 w			$\nu_{14} + \nu_{21}$	
				975 m,P	975 w	$\nu_8 + \nu_{21}$	ν_{24}
				952 m,P	950 w	ν_7	
		949 w	*				$\nu_{27} + \nu_{29}$
935 m }							
B	930 wm	927 wm	928 w			ν_{27}	
927 m }							
872 vw }	866 vw					$\nu_{10} + \nu_{28}$	
B							
862 vw }							
834 w }							
828 w *A/C*	825 wm	824 w	*				ν_{25}
821 w }							
	813 w	810 w,sh	*	815 m,P	*		ν_{10}
805 w } *B*							
780 vw }							
B				790 s,sh			$\nu_{28} + \nu_{10}$
769 vw }							
	755 w,sh	750 m	749 m			ν_{13}	
743 vw }							
737 vw,Q *A/C*							$\nu_{13} + \nu_{29}$
728 vw,Q *C*	735 wm,sh		732 w			$\nu_8 + \nu_{16}$?	
720 vw }							
B	720 wm,sh						
711 vw }							
			710 vs				
			685 vs		688 s	interac-	
			667 s		671 s	tions in	
						the crystal	
644 vs,sh }							
641 vvs,Q				650 s,br,D	651 s	ν_6, ν_{20}	ν_{11}, ν_{12}
C	648 vs,br	650 vs,br	650 s			ν_{14}, ν_{28}	ν_{26}, ν_{27}
638 vvs,Q							
634 vs,sh }							
578 m }							
571 s *A/C*	574 m	573 m	*	575 w,D	*		ν_{28}
564 m }							
483 s }			493 s				
B	484 ms	488 s	480 s	487 m,P	490 s	ν_{29}, ν_9	
475 s }			467 m,sh				
	436 w[f]	437 w	*	437 m,P	*		ν_{18}
363 m }							
353 s *C*	352 s[f]	364 s	372 s	351 m,D ?	*	ν_{15}	ν_{14}
340 m }							
320 m }							
312 s *A/C*	318 ms[f]	324 m	*	323 ms,D	326 vs	ν_{21}	ν_{29}
306 m }							

TABLE 1 (continued)

IR					Raman		Interpretation	
Vapour		Liquid	Amorphous[b] 90 K	Crystalline[c] 90 K	Liquid	Crystalline[c] 90 K	*Anti*	*Gauche*
212w 204mw 198w	*A/C*	215mw[f]	220wm	*	221s,P	226vs	ν_{10}	ν_{30}
		183vw[f]			182m,D?	*		ν_{15}
				178m				
				160m				
				143m				
				122m		123s	Lattice	
						118s	modes	
		107w,bd[f]					ν_{16},ν_{30}?	
						90vs		
				74m		80mw	Lattice	
						66vs	modes	
						51s		

[a]Weak bands outside the fundamental regions 4000—3400, 2800—2150 and 2100—1480 cm^{-1} are omitted. [b]Condensed from vapour at liquid N_2 temperatures. [c]Condensed from vapour at liquid N_2 temperatures, annealed at 190 K and recooled to liquid N_2 temperatures. [d]s, strong; m, medium; w, weak; v, very; sh, shoulder; bd, broad; P, polarized; D, depolarized; *Q*, *Q*-branch; *A*, *B*, *C*, vapour contours; comb., combination band. [e]An asterisk signifies that the band vanishes in the crystalline solid spectra. [f]Benzene solution.

(ν_{29} and ν_{30}) overlapped the Raman active *anti* fundamentals ν_{21} (b_g) and ν_{10} (a_g). In BP-d_2 exactly the same features were observed (cf. Fig. 7 and Table 2).

Our present assignments for BP are listed in Tables 1 and 3, and will be briefly discussed if they deviate from our earlier results [1]. All the a_g modes of the *anti* conformer were left unchanged. The b_g modes ν_{18} and ν_{19} were assigned to the Raman bands at 1286 and 1003 cm^{-1}, respectively, the latter coinciding with the *gauche* fundamental ν_9 (*a*). Previously, the a_u mode ν_{13} was unassigned but it is now ascribed to a distinct band at 756 cm^{-1} in the BP-d_2 spectrum, appearing as a weak shoulder in the parent IR spectrum. The b_u fundamental ν_{26} is now attributed to the intense bands at 1260 cm^{-1}, partly covered by the overtones of the C≡C—H bending modes (see below). A band at 1337 cm^{-1} previously assigned to the ν_{26} *anti* fundamental [1], is now assigned to the *gauche* mode ν_{22}.

Comparatively few *gauche* fundamentals were assigned previously. Presently, a number of observed IR and Raman bands are assigned to the *gauche* conformer when fulfilling the requirements: (a) bands vanishing in the crystal spectra, (b) bands having the expected IR vapour contours and (c) bands corresponding to the calculated wavenumbers for the appropriate *gauche* fundamental.

Two Raman bands observed at 1225 and 1030 cm^{-1} were assigned as the *a* fundamentals ν_7 and ν_8. Six new *b* fundamentals of the *gauche* conformer were assigned to observed IR and/or Raman bands: ν_{18}, ν_{19}, ν_{21}, ν_{22}, ν_{23} and ν_{24}. Our present force constant calculations indicated a number of instances in which the *anti* and *gauche* fundamentals should overlap. Additional

gauche fundamentals were assigned to bands overlapping *anti* fundamentals whenever acceptable from the various criteria.

Nearly all the *gauche* fundamentals were assigned, as is apparent from Table 3. Exceptions are two of the CH_2 stretching modes ν_2 and ν_3 as well as the torsional mode ν_{16}. Weak broad absorption bands were observed at ca. 105 cm^{-1} in the IR spectrum of BP and at 95 cm^{-1} for BP-d_2 (Fig. 12), both in concentrated benzene solutions. The bands may be attributed to the torsional mode ν_{16} eventually overlapping the lowest in-phase bending mode ν_{30} of the *anti* conformer.

Spectral assignments in BP-d_2

A comparison between Tables 1 and 2 as well as 3 and 4 reveals the striking similarities between the spectra of BP and BP-d_2. Approximately 20 of the 30 *anti* fundamentals in BP lie within 5 cm^{-1} of the corresponding fundamentals in BP-d_2. The deuterated spectrum greatly faciliated the interpretation of the parent spectrum (and vice versa).

The main spectral differences are that the acetylenic C—H stretches (coinciding for the a_g, b_u, a and b modes) are shifted from 3332 cm^{-1} in BP to 2612 cm^{-1} in BP-d_2. Correspondingly, the C≡C—H bending modes are shifted from ca. 650 to ca. 500 cm^{-1}. Also, the bands around 2120 cm^{-1} in BP (ν_3 and ν_{24} of *anti* and ν_4 and ν_{20} of *gauche*) are shifted to ca. 1985 cm^{-1} in BP-d_2. Thus, the C≡C stretch contains a significant contribution from C—H(D) stretch. The low frequency modes below 500 cm^{-1} involving various skeletal bending motions also shift slightly more than the high frequency modes (stretching) upon deuteration.

It is well known that the acetylenic C—H bending modes give rise to very intense and broad overtones in the IR and Raman, appearing at ca. 1270 cm^{-1} (vapour) for BP and around 1010 cm^{-1} for BP-d_2. In the low temperature crystal, the fundamentals as well as the overtones are found at higher wave numbers for BP as well as for BP-d_2. The *anti* fundamentals ν_{26} (1260 cm^{-1}) and ν_{18} (1286 cm^{-1}) for both compounds were partly hidden in the BP spectra but could easily be observed in the BP-d_2 spectra. The range 1020—950 cm^{-1}, partly covered in the BP-d_2 spectra, was easily interpreted for BP. The force constant calculations indicate that the fundamentals in this region (ν_6 and ν_{19}, *anti* and ν_8 and ν_9, *gauche*) should occur at approximately the same wave numbers for BP and BP-d_2. The complex spectra for BP-d_2 in this region have prevented a clear-cut identification of these bands and the modes have been left unassigned for BP-d_2.

Force constant calculations

A normal coordinate analysis was carried out with various purposes in mind. From the fairly reliable assignments of fundamentals to the *anti* and *gauche* conformers we wanted to derive a common set of force constants for

TABLE 2

IR and Raman spectral data[a] for 1,5-hexadiyne, 1,6-d_2 (dideutrobipropargyl)

IR				Raman		Interpretation	
Vapour	Liquid	Amorphous[b] 90 K	Crystalline[c] 90 K	Liquid	Crystalline[c] 90 K	*Anti*	*Gauche*
	2978 w,sh[d]		2988 vw			$\nu_{26}+\nu_{24}$	
2971 m,sh 2964 s,Q *A/C* 2959 s	2946 m,sh						ν_{17}
			2955 s				
2956 s,Q *C*	2935 m,sh	2930 m,sh		2936 s,sh	2939 vs	ν_{11},ν_{17}	
2945 s			2933 m				
2951 s					2918 vs		
B	2921 s	2918 s	2917 s	2921 vs,P		ν_{12},ν_1	
2939 s					2908 vs		
2932 s *A/C*							ν_{18}
2926 m,sh 2871 m							
B				2874 m,P	2860 w		
2866 m						comb.	
	2850 m	2843 m	2837 m				
2861 m *A/C*				2848 m,P	2830 w		
2858 m							
	2804 w,sh					$\nu_{10}+\nu_{23}$	
				2672 w,P	2670 w	$\nu_{25}+\nu_{26}$	
2617 vs			2585 w	2626 vw,P			
2612 vs *A/B*	2599 vs	2583 vs		2592 m,P	2573 m	ν_{23},ν_2	ν_3,ν_{19}
2606 vs			2570 vs				
		2559 s,sh	2558 s				
		2548 s,sh	*[e]				
		2535 m	2535 s				
	2122 w			2121 w,P	2118 w	ν_{24},ν_3 parent	
	2045 w	2036 w	2035 w			$\nu_3+\nu_{16}$?	
			1982 s		1976 vs		
	1986 s	1983 s		1983 vs,P		ν_{24},ν_3	ν_4,ν_{20}
			1973 s		1961 s		
			1945 w				
	1922 w	1920 w	1922 w			$\nu_{20}+\nu_{28}$	
				1894 w			$\nu_{22}+\nu_{26}$
			1861 w				
	1857 w	1859 w				$\nu_7+\nu_{27}$	
			1843 w				
				1825 vw,P	1822 w	$\nu_5+\nu_{20}$	
				1780 vw,P		$\nu_{18}+\nu_{20}$	
	1764 w	1756 w				$\nu_8+\nu_{26}$	
				1520 vw		$\nu_6+\nu_8$	
					1504 w	$\nu_6+\nu_{20}$	
~1490 w,sh	1490 m,sh	1490 w	1506 w			$\nu_{14}+\nu_{19}$	
			1474 w				
~1465 w,sh	1461 m,sh	1465 w	1472 w			$\nu_6+\nu_{29}$	
			1457 vw				
1447 m	1441 s,sh		1430 s			ν_{25}	
1441 s,Q *A/C*	1435 s	1435 s		1435 m,D?	1426 s	ν_4	ν_5,ν_{21}
1437 m							
		1345 mw,sh					$\nu_8+\nu_{29}$
1348 m				1344 m,P	1339 s	ν_5	
1341 m *A/C*	1337 m	1337 m	*				ν_{22}
1334 m							
B	1320 m	1318 wm	1320 w	1321 m,P	1324 w	$\nu_{16}+\nu_{26}$?	ν_6
1322 wm							

TABLE 2 (continued)

IR				Raman		Interpretation	
Vapour	Liquid	Amorphous[b] 90 K	Crystalline[c] 90 K	Liquid	Crystalline[c] 90 K	*Anti*	*Gauche*
~1290 vvw		1290 w	*	1287 w,D	1289 m	ν_{18}	$\nu_{10}+\nu_{12}$
1266 s			1256 s				
1260 s *A/B*	1260 s	1258 s				ν_{26}	
1256 s			1254 s				
~1240 w,sh	1232 w	~1233 w	*	1230 m,P	*		ν_{7}
		~1220 w	*				$\nu_{13}+\nu_{25}$
1203 vw							
1190 vw,Q *C*	1188 m	1187 mw	1197 m			ν_{12}	
1182 vw							
1175 vw,Q *A/C*				1186 w,D	*		ν_{23}
1170 vw							
1130 vw	1125 w		~1130 vw			$\nu_{10}+\nu_{27}$	
			1085 s				
			1071 m			comb. of	
	1064 m,sh					interac-	
						tion in	
						the	
						crystal	
			1055 m				
1044 w			1038 s				
B	1032 s,sh	1033 ms,br					
1036 w			1030 s				
1025 m							
1020 m *A/B*?			1024 m			comb.	
1015 m							
1012 m							
B	1007 s	1011 s	1011 s	1010 m,P	1010 s		
1003 m							
985 s,br	990 s,sh	990 m,sh	990 w				
	963 m,sh	961 w	*				ν_{24}?
					955 m		
				949 m,P		ν_{7}	
					935 m,sh		
	941 m,sh					$\nu_{9}+\nu_{14}$	
933 m							
B	915 m,sh	912 w	912 w			ν_{27}	
925 m							
		875 w,bd	876 w	875 vw			
	848 vw,sh					$\nu_{8}+\nu_{18}$	
830 w							
822 w *A/C*	820 m	817 w	832 w,bd	830 vw,sh		$\nu_{16}+\nu_{20}$	ν_{25}
816 vw							
801 w							
B	805 vw,sh			802 m,P	*		ν_{10}
793 w							
768 vw							
B							$\nu_{26}+\nu_{30}$
756 vw							
	756 w	753 m	747 s			ν_{13}	
736 vw							
730 vw *A/C*							$\nu_{15}+\nu_{26}$
722 w							
B						$\nu_{10}+\nu_{28}$	
712 vw							
		696 w	698 m				

TABLE 2 (continued)

IR					Raman		Interpretation	
Vapour		Liquid	Amorphous[b] 90 K	Crystalline[c] 90 K	Liquid	Crystalline[c] 90 K	*Anti*	*Gauche*
644 w								
				667 w		682 vw,bd		
641 w							ν_8, ν_{14}, ν_{20}, ν_{28}	
	C	648 m	663 m,bd	664 m	650 vw,bd		parent	
638 w						632 vw,bd		
				648 w,bd				
634 w								
577 m								
571 m	*A/C*	574 m	575 m	*	575 w,D	*		ν_{26}
565 m								
				549 vs		555 vs	interac-	
				537 vs		536 vs	tions in	
				517 s,sh		517 vs	the crystal	
					514 s,bd,D	508 vs	ν_8, ν_{20}	
507 vs		508 s,sh[f]					ν_{28}	
	C,B							ν_{11}, ν_{12}, ν_{27}, ν_{28}
503 vs			507 vs,bd	511 vs				
497 vs,*Q*		497 vs[f]					ν_{14}	
466 s				482 vs				
	B	466 s[f]	470 vs				ν_{29}	
459 s				469 vs				
						486 vw		
					463 m,P		ν_9	
						469 m		
		420 w[f]	425 w	*	419 m,P	*		ν_{13}
350 s								
342 s	*C*	341 s[f]	352 s	363 s	338 m,D?	*	ν_{15}	ν_{24}
~330 s								
307 m								
300 s	*A/C*	307 s[f]	313 m	*	306 m,D	312 s	ν_{21}	ν_{29}
293 m								
						219 m		
					207 s,D?		ν_{10}	
						211 s		
201 w								
194 w	*A/C*	203 w[f]	210 w	*				ν_{30}
187 w								
					172 m,D?	*		ν_{15}
			168 w	170 m				
			147 w	148 m				
			134 w	136 m			Lattice	
			115 w	116 m		117 s	modes	
		95 vw,bd[f]					ν_{16}, ν_{30}	
						82 s		
			70 m	74 m			Lattice	
						58 s	modes	
						48 m		

[a]Bands above 3000 cm^{-1} and weak bands in the region 2500—2200 cm^{-1} are omitted. [b]Condensed from vapour at liquid N_2 temperatures. [c]Condensed from vapour at liquid N_2 temperatures, annealed at 190 K and recooled to liquid N_2 temperatures. [d]s, strong; m, medium; w, weak; v, very; sh, shoulder; bd, broad; P, polarized; D, depolarized; *Q*, *Q*-branch; *A*, *B*, *C*, vapour contours; comb., combination band. [e]An asterisk signifies that the band vanishes in the crystalline solid spectra. [f]Benzene solution.

TABLE 3

Observed[a] and calculated fundamental frequencies (cm^{-1}) for 1,5-hexadiyne

	Anti conformer				*Gauche* conformer		
	Obs.	Calc.	PED[b]		Obs.	Calc.	PED
a_g				a			
ν_1	3332[c]	3346	96r[d]	ν_1	3332[c]	3346	96r
ν_2	2921[e]	2935	99s	ν_2		2964	98s
ν_3	2118	2120	83d	ν_3		2934	98s
ν_4	1436	1421	80ρ	ν_4	2121	2122	83d
ν_5	1346	1355	$57\delta' + 39\delta + 15$p	ν_5	1435[e]	1427	80ρ
ν_6	1022	1023	91h	ν_6	1321	1318	$60\delta + 32\delta'$
ν_7	952	947	45p $+ 36\omega$	ν_7	1225	1214	$61\delta' + 42\delta + 15$h
ν_8	650	647	111ϕ	ν_8	1030[c]	1021	81h
ν_9	487	483	$35\omega + 23\theta + 20$p	ν_9	1002	992	$44\delta' + 29\delta$
ν_{10}	221	217	$92\theta + 17\omega$	ν_{10}	815	823	57p $+ 15\delta$
a_u				ν_{11}	648	648	$110\phi'$
ν_{11}	2956[c]	2958	99s	ν_{12}	648	646	111ϕ
ν_{12}	1191[c]	1193	$74\delta' + 25\delta$	ν_{13}	436	433	$45\omega + 42\theta$
ν_{13}	756	754	$72\delta + 19\delta'$	ν_{14}	351	346	$94\theta'$
ν_{14}	648	648	$110\phi'$	ν_{15}	182	185	$63\theta + 30\omega$
ν_{15}	352	351	$98\theta'$	ν_{16}		73	71τ
ν_{16}		71	80τ	b			
b_g				ν_{17}	3332[c]	3346	96r
ν_{17}	2938[e]	2966	99s	ν_{18}	2964[c]	2962	98s
ν_{18}	1287	1290	$71\delta + 28\delta'$	ν_{19}	2932[c]	2932	98s
ν_{19}	1003	1003	$69\delta' + 26\delta$	ν_{20}	2121	2124	83d
ν_{20}	650	648	$110\phi'$	ν_{21}	1435	1445	$76\rho + 22\delta'$
ν_{21}	323	319	$112\theta'$	ν_{22}	1338	1335	$54\delta + 34\delta'$
b_u				ν_{23}	1181[c]	1180	$62\delta' + 38\delta$
ν_{22}	3332[c]	3346	96r	ν_{24}	975	989	32p $+ 28\delta' + 20\omega$
ν_{23}	2921[e]	2930	99s	ν_{25}	825	822	47p $+ 29\delta$
ν_{24}	2121	2125	83d	ν_{26}	648	648	$107\phi'$
ν_{25}	1441	1446	$77\rho + 20\delta'$	ν_{27}	648	648	107ϕ
ν_{26}	1260	1265	$47\delta + 45\delta'$	ν_{28}	574	580	$52\omega + 23\delta + 20\theta$
ν_{27}	930	927	82p	ν_{29}	318	322	$111\theta'$
ν_{28}	648	648	110ϕ	ν_{30}	215	214	$96\theta + 15\omega$
ν_{29}	484	474	$52\omega + 49\theta$				
ν_{30}		132	$69\theta + 39\omega$				

[a]When possible frequencies are taken from liquid or solution spectra. [b]The potential energy distribution is defined as $\chi_{ik} = 100\ F_{ii}L_{ik}^2/\lambda_k$. [c]Frequencies from the vapour phase spectrum. [d]For meaning of symbols see Fig. 1. Terms below 15 are neglected. [e]Not included in the refinement of the force constants.

both conformers. It was clear from our earlier work in which a diagonal force field with 11 independent force constants was employed [1] that a considerable number of interaction constants had to be included in order to improve the agreement.

TABLE 4

Observed[a] and calculated fundamental frequencies (cm^{-1}) for 1,5-hexadiyne-1,6-d_2

	Anti conformer			*Gauche* conformer		
	Obs.	Calc.	PED[b]	Obs.	Calc.	PED
a_g				a		
ν_1	2921[c]	2935	99s[d]	ν_1	2964	98s
ν_2	2612[e]	2595	70r + 27d	ν_2	2934	98s
ν_3	1983	1986	58d + 28r	ν_3	2612[e]	2596	70r + 27d
ν_4	1435	1421	80ρ	ν_4	1986	1987	58d + 28r
ν_5	1344	1354	57δ + 39δ'	ν_5	1435[c]	1427	80ρ
ν_6		1022	93h	ν_6	1320	1318	60δ + 32δ'
ν_7	949	939	44p + 36ω	ν_7	1225	1214	61δ' + 42δ + 15h
ν_8	514	513	94ϕ + 20θ	ν_8		1019	84h
ν_9	463	461	25ω + 22ϕ	ν_9		990	43δ' + 30δ
ν_{10}	207	208	89θ + 16ω	ν_{10}	805	814	58p + 15δ
a_u				ν_{11}	497[c]	507	97ϕ + 15ϕ'
ν_{11}	2956[e]	2958	99s	ν_{12}	497[c]	503	101ϕ' + 15ϕ
ν_{12}	1190[c]	1193	74δ' + 25δ	ν_{13}	420	422	41ω + 28θ
ν_{13}	756	754	72δ + 19δ'	ν_{14}	338	336	84θ'
ν_{14}	497	504	116ϕ'	ν_{15}	172	178	63θ + 29ω
ν_{15}	341	341	90θ'	ν_{16}		62	70τ
ν_{16}		68	79τ	b			
b_g				ν_{17}	2964[e]	2962	98s
ν_{17}	2936[c]	2966	99s	ν_{18}	2932[e]	2932	98s
ν_{18}	1287	1290	71δ + 28δ'	ν_{19}	2612[e]	2596	70r + 27d
ν_{19}		1002	69δ' + 26δ	ν_{20}	1986	1989	58d + 28r
ν_{20}	514[c]	503	116ϕ'	ν_{21}	1435	1445	76ρ + 22δ'
ν_{21}	306	307	105θ'	ν_{22}	1337	1334	53δ + 35δ'
b_u				ν_{23}	1175[e]	1179	62δ' + 38δ
ν_{22}	2921[c]	2930	99s	ν_{24}	963[c]	983	29p + 29δ' + 20ω
ν_{23}	2612[e]	2596	70r + 27d	ν_{25}	820	814	48p + 28δ
ν_{24}	1986	1990	58d + 28r	ν_{26}	574	581	51ω + 23δ + 22θ
ν_{25}	1441	1446	77ρ + 20δ'	ν_{27}	497[c]	503	110ϕ'
ν_{26}	1260	1264	48δ' + 45δ	ν_{28}	497[c]	498	103ϕ
ν_{27}	915	915	80p	ν_{29}	307	311	103θ'
ν_{28}	508	508	108ϕ + 23θ	ν_{30}	203	204	93θ
ν_{29}	466	463	44ω + 28θ				
ν_{30}		124	69θ + 37ω				

[a]When possible frequencies are taken from liquid or solution spectra. [b]The potential energy distribution is defined as $\chi_{ik} = 100\ F_{ii}L_{ik}^2/\lambda_k$. [c]Not included in the refinement of the force constants. [d]For meaning of symbols see Fig. 1. Terms below 15 are neglected. [e]Frequencies from the vapour phase spectrum.

The notation of the applied valence coordinates is defined in Fig. 13. The structural parameters were taken as follows: $r = 1.065$, $d = 1.220$, $p = 1.459$, $h = 1.555$ and $s = 1.095$ Å, $\theta = \phi = 180$, $\omega = 110.7$, $\rho = 110.2$, $\delta = 108.7$ and $\tau = 180°$ (77 *gauche*). The initial diagonal valence force field [1] was

TABLE 5

Calculated relative integrated infrared intensities for the methylene stretching vibrations in 1,5-hexadiyne-1,6-d_2

Fundamental	Frequency	Contour	Relative intensity
ν_{11} a_u *anti*	2956	*C*-type	3.02
ν_{22} b_u *anti*	2942	$I_A/I_B = 8.7$	1.36
ν_i *a gauche*	2964[a]	*B*-type	0.76
ν_2 *a gauche*	2934[a]	*B*-type	0.70
ν_{17} *b gauche*	2964	$I_C/I_A = 2.7$	2.26
ν_{16} *b gauche*	2932	$I_C/I_A = 5.9$	0.66

[a]Estimated from normal coordinate analysis.

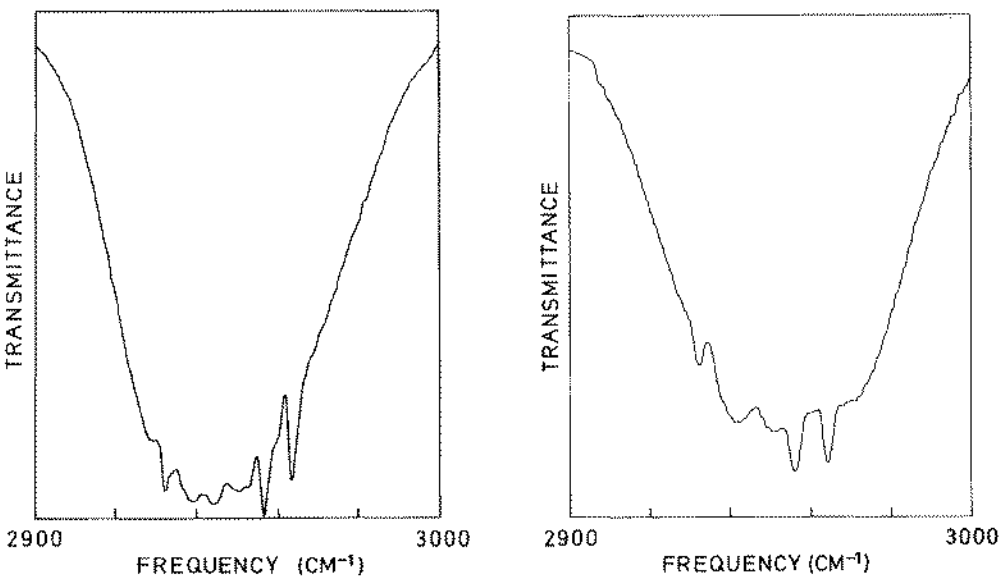

Fig. 10. The observed CH_2 stretching bands of BP-d_2 in the vapour phase; 20 cm path, 39 torr pressure.

Fig. 11. The computed CH_2 stretching bands of BP-d_2 (see Table 5).

extended by transferring the interaction constants found for the n-alkanes [13]. Only minor adjustments were necessary in order to obtain an excellent agreement with the experimental observations as shown in Tables 3 and 4 for BP and BP-d_2, respectively. On the average, the deviation is better than 1%.

The final force field is given in Table 6 and consists of 35 parameters of which 13 were constrained to their values in the n-alkanes [13] during the least squares refinement. As seen, practically all the force constants are well

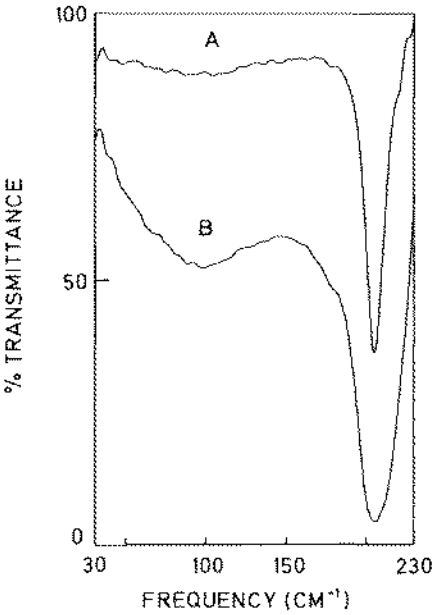

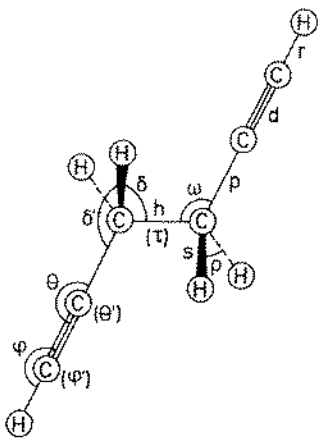

Fig. 12. The far infrared spectrum of BP-d_2 dissolved in benzene; A, 11% solution; B, 66% solution; 1 mm cell of polyethylene.

Fig. 13. The valence coordinates of BP (*anti* conformer).

determined and have the correct magnitudes. As noted in Tables 3 and 4 some of the assigned fundamental frequencies were not employed in the refinement procedure. However, all together 91 fundamental frequencies of the *anti* and *gauche* fundamentals of BP and BP-d_2 were used to determine the 22 force constants which were not constrained.

The potential energy distribution (PED) in Tables 3 and 4 reveals that many of the modes are fairly well localized to one internal coordinate. Moreover, the "corresponding" vibrational modes are frequently equally well localized in the BP and BP-d_2 spectra for both *anti* and *gauche*.

Solid state spectra

As reported [1] the shock-frozen solid condensed from the vapour on a CsI plate or on a copper block at 90 K contained both conformers, while the annealed crystalline solid contained only the *anti* conformer (Figs. 6 and 7). At higher temperatures (200—260 K), but below the melting point at 267 K certain spectral changes of band width and intensities were observed, suggesting a phase transition in this region. By differential scanning calorimetry (DSC) a sharp peak indicating a first order phase transition was observed at ca. 240 K. Semiquantitative DSC measurements gave a ΔH value for the phase transition equal to —0.6 kcal mol^{-1} and a ΔS equal to —2.6 cal mol^{-1} K.

TABLE 6

Valence force constants for 1,5-hexadiyne

Force constant	Group	Coordinate(s) involved	Atoms common to interacting coordinates	Calculated value ϕ_i	Standard error $\sigma(\phi_i)$
Stretch[a]				mdyn Å^{-1}	
K_s	—CH_2—CH_2—	C—H	—	4.737	0.035
K_t	—C≡C—H	C—H	—	5.983	0.044
K_d	—C≡C—H	C≡C	—	15.22	0.14
K_p	CH_2—C≡C	—C—C≡	—	5.138	0.065
K_h	CH_2—CH_2	C—C	—	4.87	0.17
Bend				mdyn Å rad^{-2}	
H_ρ	CH_2—CH_2	HCH	—	0.5385	0.0049
H_δ	CH_2—CH_2	HCC	—	0.6464	0.0083
$H_{\delta'}$	C≡C—CH_2	CCH	—	0.6734	0.0089
H_ϕ, $H_{\phi'}$	C≡C—H	CCH	—	0.2348	0.0020
H_θ	C≡C—CH_2	CCC	—	0.2933	0.0042
$H_{\theta'}$	C≡C—CH_2	CCC	—	0.3317	0.0031
H_ω	C—CH_2—CH_2	CCC	—	1.143	0.019
Torsion[b]				mdyn Å rad^{-2}	
τ	CH_2—CH_2	HCCH	—	0.0314	0.0023
Stretch-stretch				mdyn Å^{-1}	
F_s	CH_2—CH_2	C—H, C—H	C	0.080	0.036
F_{hp}	CH_2—CH_2—C≡	C—C, C—C≡	C	0.577	0.088
Stretch-bend				mdyn rad^{-1}	
$F_{p\omega}$	CH_2—CH_2—C	C—C≡, CCC	C—C	0.524	0.052
$F_{h\omega}$	CH_2—CH_2—C	C—C, CCC	C—C	0.686	0.094
$F_{h\delta}$	CH_2—CH_2	C—C, HCC	C—C	0.350	0.015
$F_{p\delta'}$	C≡C—CH_2	C—C, CCH	C—C		
$F_{h\delta'}$	≡C—CH_2—CH_2—	—C—C—, ≡CCH	C	0.079	—[c]
$F_{p\delta}$	≡C—CH_2—CH_2—	≡C—C, HCC—	C		
Bend-bend				mdyn Å rad^{-2}	
$F_{\phi\theta}$	CH_2—C≡C—H	CCH, CCC	C≡C	0.1102	0.0043
$F_{\omega\delta}$	≡C—CH_2—CH_2—	CCC, HCC—	—C—C—	—0.031	—
$F_{\omega\delta'}$	≡C—CH_2—CH_2—	CCC, ≡CCH	≡C—C	—0.031	—
F_δ	CH_2—CH_2	HCC, HCC	C—C	—0.021	—
$F_{\delta'}$	≡C—CH_2	CCH, CCH	C—C	—0.021	—
$F_{\delta\delta'}$	≡C—CH_2—CH_2—	≡CCH, HCC—	C	0.012	—
f^t_ω	C—CH_2—CH_2—C	CCC, CCC	(C)—C —*trans*— C—(C)	0.026	0.026
f^g_ω	C—CH_2—CH_2—C	CCC, CCC	(C)—C —*gauche*— C—(C)	—0.200	0.019
$f^t_{\omega\delta}$	CH_2—CH_2—C	CCC, HCC	(H)—C —*trans*— C—(C)	0.049	—
$f^g_{\omega\delta}$	CH_2—CH_2—C	CCC, HCC	(H)—C —*gauche*— C—(C)	—0.052	—
f^t_δ	CH_2—CH_2	H_aCC, H_bCC	(H_a)—C —*trans*— C—(H_b)	0.1151	0.0065
f^g_δ	CH_2—CH_2	H_aCC, H_bCC	(H_a)—C —*gauche*— C—(H_b)	—0.005	—
$f^t_{\delta\delta'}$	CH_2—CH_2—C≡	H_aCC—, H_bCC≡	(H_a)—C —*trans*— C—(H_b)	0.002	—
$f^g_{\delta\delta'}$	CH_2—CH_2—C≡	H_aCC—, H_bCC≡	(H_a)—C —*gauche*— C—(H_b)	0.009	—
$f^t_{\delta'}$	≡C—CH_2—CH_2—C≡	H_aCC—, HCC_b≡	(H_a)—C —*trans*— C—(C_b≡)	—0.014	—
$f^g_{\delta'}$	≡C—CH_2—CH_2—C≡	H_aCC—, HCC_b≡	(H_a)—C —*gauche*— C—(C_b≡)	—0.025	—

[a]Internal coordinates and symbols are defined in Fig. 1. [b]The torsion is defined as a normalized sum of three *trans*-torsions. [c]Values from ref. 13.

The corresponding values for the melting were $\Delta H = -2.6$ kcal mol^{-1} and $\Delta S = -9.6$ cal mol^{-1} K.

Complete mid-IR spectra were recorded for every five degrees in the range 280 to 200 K (passing the melting point at 267 K) of BP in a sandwich cell, by means of the Fourier transform spectrometer. The liquid state spectra above 270 K were essentially identical to those at ambient temperature, with slightly sharper bands. At ca. 265 K the *gauche* bands practically vanished and the spectrum remained the same until 240 K. Below this temperature, the spectrum still consists of *anti* bands. In addition, an intense band appeared around 1377 cm^{-1}, similar to the 90 K spectrum (Fig. 2 of ref. 1), except that sharp peaks at 1412, 1392, 1383, 1344 and 1315 cm^{-1} (Table 1) were resolved in the latter spectrum. These bands are attributed to overtones and combination bands of ν_8, ν_{14}, ν_{20} and ν_{28} of the *anti* conformer in the crystalline state. Upon heating, the 1377 cm^{-1} band disappeared around 240 K but the *gauche* bands did not return before melting at 270 K.

Thus, the high temperature solid phase of BP (phase I, above 240 K) consists of molecules in the *anti* conformer, as in the low temperature phase (phase II, below 240 K). Various reversible spectral changes occurred in the *anti* bands on going from phase I to phase II at ca. 240 K, but the appearance of the 1377 cm^{-1} band (and the bands around 685 cm^{-1}) were most prominent.

BP was further crystallized at ambient temperature in a high pressure diamond anvil cell, frequently employed for conformational studies in our laboratory [14]. At ca. 1—2 kbar (estimated pressure) the liquid crystallized probably into phase I and the *gauche* bands disappeared. At ca. 5—10 kbar a phase transition (probably into phase II) could be visually observed in a polarization microscope. The *anti* bands were still present and the 1380 cm^{-1} band appeared. No further phase transitions at higher pressures were detected.

The low temperature (and high pressure) solid of BP was accordingly different from those of 1,2-dicyanoethane [15, 16] and 1-cyano-3-butyne [7]. In 1,2-dicyanoethane a reversible phase transition occured at 223 K [15]; below this temperature the *gauche* conformer was stable, above an *anti*—*gauche* equilibrium existed, indicating that the high temperature phase was plastic (cubic). 1-Cyano-3-butyne, on the other hand, had a stable crystal, containing what was believed to be the *anti* conformer. However, an apparently metastable crystal could be formed by annealing the amorphous solid from 90 K to ca. 140 K, containing the *gauche* conformer [7]. When the *anti* conformer was formed, however, we were unable to reform the *gauche* conformer [7], indicating an irreversible transition. At high pressure only the *anti* conformer of 1-cyano-3-butyne was detected. Accordingly, these three isoelectronic molecules i.e. BP, 1-cyano-3-butyne and 1,2-dicyanoethane, of which 1-cyano-3-butyne can be considered a hybrid of the others, have quite different conformational features in the solid. Although the three compounds are isoelectronic, the crystals are probably greatly influenced by the vast difference in dipole moments between the C≡C—H and C≡N groups.

ACKNOWLEDGEMENT

The authors are grateful to G. Isaksen for performing the differential scanning calorimetry measurements and to E. Tørneng who recorded the high pressure spectra. Financial support from the Norwegian Research Council for Science and the Humanities is acknowledged.

REFERENCES

1 D. L. Powell, P. Klaeboe, A. Phongsatha, B. N. Cyvin, S. J. Cyvin and H. Hopf, J. Mol. Struct., 41 (1977) 203.
2 C. Binet and R. Romanet, J. Raman Spectrosc., 5 (1976) 243.
3 M. Traetteberg, P. Bakken, R. Seip, S. J. Cyvin, B. N. Cyvin and H. Hopf, J. Mol. Struct., 51 (1979) 77.
4 A. Phongsatha, P. Klaeboe, B. N. Cyvin, S. J. Cyvin and H. Hopf, J. Mol. Struct., 43 (1978) 1.
5 D. L. Powell, P. Klaeboe, B. N. Cyvin and H. Hopf, J. Mol. Struct., 41 (1977) 215.
6 D. L. Powell, P. Klaeboe, B. N. Cyvin and H. Hopf, J. Mol. Struct., 43 (1978) 193.
7 P. Klaeboe, M. Moneeb, E. Tørneng, H. Hopf, I. Böhm, B. N. Cyvin and S. J. Cyvin, Z. Naturforsch., Teil A, 35 (1980) 537.
8 P. Klaeboe and T. Woldbaek, Appl. Spectrosc., 32 (1978) 588.
9 B. Gilbert and G. Duyckaerts, Spectrochim. Acta, Part A, 26 (1970) 2197.
10 T. Ueda and T. Shimanouchi, J. Mol. Spectrosc., 28 (1968) 350.
11 W. A. Seth-Paul, J. Mol. Struct., 3 (1969) 403.
12 W. J. Orville-Thomas, S. Suzuki and G. Riley, in A. J. Barnes and W. J. Orville-Thomas (Eds.), Vibrational Spectroscopy — Modern Trends, Elsevier, Amsterdam, 1977, p. 167.
13 R. G. Snyder and J. H. Schachtschneider, Spectrochim. Acta, 21 (1965) 169.
14 P. Klaeboe, Opt., Pura Appl. (Madrid), 11 (1978) 137.
15 W. E. Fitzgerald and C. J. Janz, J. Mol. Spectrosc., 1 (1957) 49.
16 T. Fujiyama, K. Tokumaru and T. Shimanouchi, Spectrochim. Acta, 20 (1964) 415.